Formation of Crystalline Ag_xNi_{1-x} Solid Solutions of Unusually High Supersaturation by Laser Ablation Deposition

R. P. van Ingen,[1,2,*] R. H. J. Fastenau,[1] and E. J. Mittemeijer[2]

[1]*Philips Research Laboratories, Prof. Holstlaan 4, 5656 AA Eindhoven, The Netherlands*

[2]*Laboratory of Materials Science, Delft University of Technology, Rotterdamseweg 137, 2628 AL Delft, The Netherlands*

(Received 21 December 1993)

Laser ablation was used in a vapor quenching method to deposit thin Ag-Ni films at room temperature. The films contained substantial amounts of a polycrystalline nonequilibrium Ag_xNi_{1-x} solid solution, as evidenced by x-ray and electron diffraction. The unusually high degree of supersaturation attained (up to 44 at.% Ag) has not been observed before for a system exhibiting such a strong demixing behavior. The x-ray diffraction $\sin^2\psi$ method was employed to determine the strain-free lattice parameter of the solid solution. The solid solution decomposed by heating the film.

PACS numbers: 81.15.Ef, 61.10.−i, 64.75.+g

Laser ablation deposition (LAD) was used to grow thin films of a variety of materials [1]. This physical vapor deposition technique owes its interest to the following characteristics. Laser ablation is possible for many materials, because most materials turn optically opaque due to high-power laser radiation-induced optical breakdown [2]. Laser ablation proceeds congruently [3], that is, none of the constituent elements of the target vaporizes preferentially. This can result in the deposition of a film with a composition equal to that of the target; however, this is not always the case [4,5]. LAD is associated with a very high quenching rate and a very high instantaneous deposition rate. The quenching rate is of the same order of magnitude as in the case of sputter deposition ($\sim 10^6$ Ks^{-1} [6]), because the kinetic energies of laser ablated species [1,2] are of the same order of magnitude as those of sputtered species [6]. The instantaneous growth rate during LAD ($\sim 8\times10^{-3}$ nm per laser pulse, corresponding to $\sim$800 nms^{-1} [5]), however, is substantially higher than the growth rate during sputter deposition ($\sim$10 nms^{-1} [6]). These properties were used here to form polycrystalline Ag_xNi_{1-x} solid solutions of a very high degree of supersaturation, which has not been reported before. Note that the equilibrium Ag-Ni phase diagram [7] shows that distinct solid solubility of either Ag in Ni or Ni in Ag cannot occur.

Upon quenching atoms in a state of high mobility, they can be "frozen" into unconventional positions and a thermodynamically metastable, or unstable, phase can develop [8]. Thus, the formation of nonequilibrium phases can be realized. In a mixture of atoms of more than one element, solid solubility limits may be surpassed and a supersaturated alloy may be formed [9,10]. Two well known rapid quenching methods are the liquid quenching method [9], as melt spinning [11] and pulsed laser surface alloying [12], and the vapor quenching method [6], including, for example, sputter deposition [13].

A liquid quenching method cannot be used to form a concentrated crystalline Ag_xNi_{1-x} solid solution, because Ag and Ni are mutually insoluble not only in the solid state, but also in the liquid state [7]. Then a vapor quenching method may be utilized to form such alloys. Thus far, sputter deposition and coevaporation of Ag and Ni on liquid-nitrogen cooled substrates have been used to form concentrated *amorphous* Ag_xNi_{1-x} alloys [13–15]. Now, this Letter reports the preparation of *crystalline* concentrated Ag_xNi_{1-x} solid solutions, with Ag contents of up to 44 at.%, by employing LAD.

The experimental setup and procedures are described only briefly here; for more details, see [5]. Target material was ablated and deposited on substrates in a turbomolecular-pumped processing chamber with a base pressure of about 5×10^{-9} mbar. Because of the nonmiscibility of liquid Ag and Ni, the Ag-Ni targets could not be prepared by arc melting. Instead, they were made by cold-pressing pure Ag and pure Ni powder mixtures into pellets. The composition of the targets was determined with x-ray fluorescence (XRF); the target compositions were 25Ag-75Ni, 50Ag-50Ni, 75Ag-25Ni, and 90Ag-10Ni, where the numbers indicate the atomic percentages of the constituent elements. To limit target degradation, the targets were rotated during ablation. The targets were ablated by laser pulses (wavelength: 193 nm; pulse width: 15 ns) from an ArF excimer laser operating at 10 Hz. The fluence (energy per unit area per pulse) used was approximately 6.0 Jcm^{-2}; fluences of about 3.0 and 7.5 Jcm^{-2} yielded similar results. The deposition rate for a fluence of 6.0 Jcm^{-2} was about 8 pm per laser pulse. The substrates were Si(100) slabs covered with a thermally grown 500-nm-thick silicon oxide film. During deposition the substrates were at room temperature. To obtain films with a homogeneous thickness, the substrates were moved in a scanning mode parallel to the targets through the laser-produced plasmas. The thicknesses of the films deposited were 100 and 500 nm. The gross compositions of the films were determined using XRF.

Identification of the phases in the thin films was achieved by x-ray diffraction (XRD) analysis. Diffraction patterns were recorded from $2\theta=10°$ to 160° on a diffractometer employing Cu $K\alpha$ radiation. From the Bragg angles of the reflections of the phases the lattice parameters of the phases present can be determined.

0031-9007/94/72(19)/3116(4)$06.00

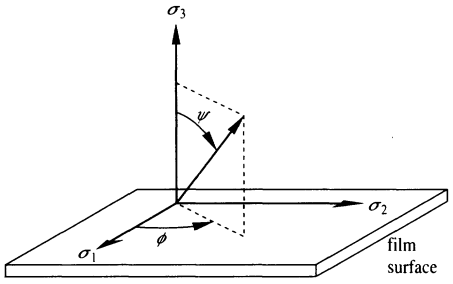

FIG. 1. Definition of the Euler angles ϕ and ψ and of the principal stress components with respect to the specimen surface.

However, if the thin film considered is stressed, the lattice spacings measured from the peak positions are affected by the (residual) stress present. To assess the magnitude of this effect and in order to perform an appropriate correction the so-called XRD $\sin^2\psi$ method [16] was used to determine the state of stress. This method allows determination of a strain-free lattice spacing as follows.

For the thin films considered a biaxial state of stress is expected with the principal stresses σ_1 and σ_2 equal to each other and parallel to the film surface. The lattice spacing d_ψ in a direction defined by the Euler angle ψ with respect to the sample reference frame, as shown in Fig. 1, obeys (with $\sigma_\parallel \equiv \sigma_1 = \sigma_2$)

$$d_\psi = d_0 + 2S_1 d_0 \sigma_\parallel + \tfrac{1}{2} S_2 d_0 \sigma_\parallel \sin^2\psi , \quad (1)$$

where ψ is the angle between the normal of the diffracting set of lattice planes (hkl) and the normal of the specimen surface, S_1 and $\frac{1}{2}S_2$ are the so-called x-ray elastic constants, and d_0 is the strain-free lattice spacing. Thus, a plot of d_ψ vs $\sin^2\psi$ should provide a straight line. From its slope a value of $\sigma_\parallel$ can be obtained, provided $\frac{1}{2}S_2$ and d_0 are known. An accurate value for $\sigma_\parallel$ can be obtained by replacing d_0 in the expression for the slope by the experimental $d_{\psi=0}$, as the latter does not deviate from d_0 by more than 1%. From Eq. (1) it follows that there exists a unique direction (ψ_0) for which $d_\psi = d_0$:

$$\sin^2\psi_0 = -2S_1/\tfrac{1}{2}S_2 . \quad (2)$$

Hence, interpolation in the plot of d_ψ vs $\sin^2\psi$ at $\psi = \psi_0$ provides a value for the strain-free spacing d_0.

For Ag_xNi_{1-x} solid solutions $2S_1$ and $\frac{1}{2}S_2$ are unknown. Therefore, here the estimates $S_1 = -\nu/E$ and $\frac{1}{2}S_2 = (1+\nu)/E$ will be applied, where ν and E are the Poisson's ratio and the Young's modulus of the film material, respectively [16]; the respective linear composition weighted values for 26Ag-74Ni (see below) are 0.35 and 1.70 GPa (using data for ν and E from [17]).

This method was applied to Ag_xNi_{1-x} {222} line profiles measured on a diffractometer employing Cu $K\alpha$ radiation, from $2\theta = 91.0°$ to 94.0°, at $\psi = 0°$ and 39.23°.

XRD patterns taken from fresh target surfaces showed that the targets were polycrystalline and composed of pure Ag and pure Ni grains, as expected. Patterns of target surfaces that had been subjected to prolonged laser irradiation were identical to those of the fresh targets. No reflections of additional phases were discernable. Although the depth of a laser-produced melt in a metal target is limited to only several tens of nanometers [3], the surface sensitive XRD method employed would detect phases that might have been formed by laser-induced alloying. Hence, significant surface alloying did not take place. It is concluded that the irradiated material was not mixed (as in a solid solution) before it was ablated to form a plasma.

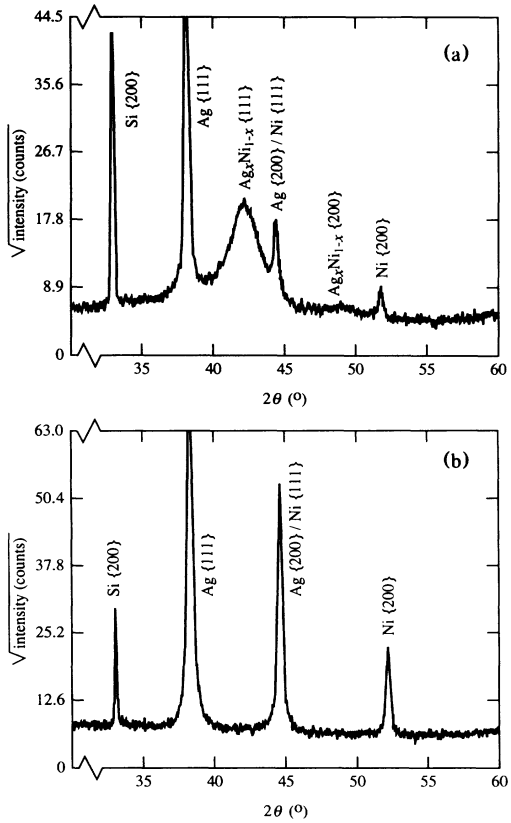

FIG. 2. (a) An XRD pattern of a 100-nm-thick 26Ag-74Ni film, showing a prominent {111} reflection of a Ag_xNi_{1-x} solid solution. (b) An XRD pattern of the 100-nm-thick 26Ag-74Ni film that was heated to 673 K at a rate of 1 K min^{-1}. The Ag_xNi_{1-x} {111} reflection has disappeared in favor of the pure Ag and pure Ni reflections, indicating that the solid solution has decomposed by the heat treatment. The Si {200} reflection in both diffraction patterns originated from the Si (100) substrate.

The gross composition of the films grown by ablation of the 25Ag-75Ni, 50Ag-50Ni, 75Ag-25Ni, and 90Ag-10Ni targets were 14Ag-86Ni, 26Ag-74Ni, 44Ag-56Ni, and 78Ag-22Ni, respectively (XRF analysis). The fact that the overall film compositions were not equal to the target compositions can be ascribed to preferential reflection of ablated Ag species at the growing film surfaces [5].

An XRD pattern of a 26Ag-74Ni film produced by LAD is shown in Fig. 2(a). The film was polycrystalline,

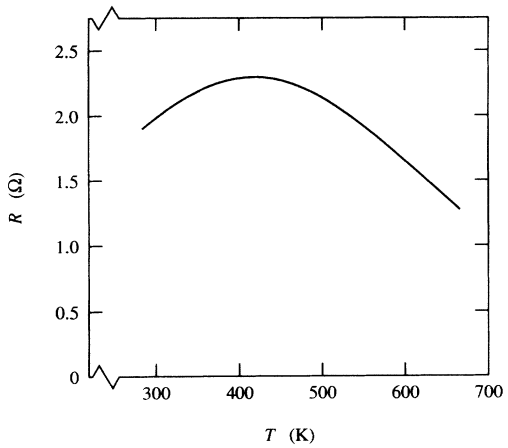

FIG. 3. The resistance R of the 100-nm-thick 26Ag-74Ni film as a function of temperature during heating the specimen from room temperature to 673 K at a rate of 1 K min^{-1}.

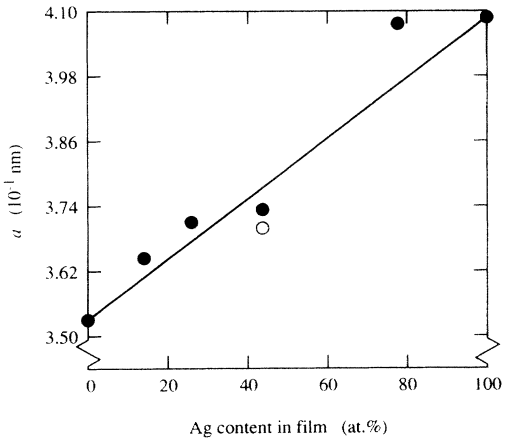

FIG. 4. The lattice parameter of the Ag_xNi_{1-x} solid solution, a, as a function of the gross Ag content of the film. The as-measured, strained values are shown for the 14Ag-86Ni, 26Ag-74Ni, 44Ag-56Ni, and 78Ag-22Ni films (●). The value after correction for the presence of residual stress (see text) is shown for the 26Ag-74Ni film (○). The straight line represents the lattice parameters that can be expected according to Vegard's law.

but not composed of a single phase. In addition to reflections originating from pure Ag and pure Ni, the diffractogram shows a prominent reflection at a Bragg angle of approximately 40° that can be interpreted as the {111} reflection of an fcc phase with a lattice parameter in between those of pure Ag and pure Ni. Other (weak) reflections of this phase could be observed too. These results were confirmed by electron diffraction analysis. The fcc phase was identified as a Ag_xNi_{1-x} solid solution. To our knowledge, this is the first time that the formation of such a nonequilibrium phase (at room temperature) is reported.

The 26Ag-74Ni film was heated in vacuum at about 10^{-7} mbar to a temperature of 673 K at a rate of 1 K min^{-1}. The XRD pattern recorded thereafter is shown in Fig. 2(b). Clearly, by heating the reflection of the solid solution disappeared entirely and the reflections of pure Ag and pure Ni gained intensity. Hence, the heat treatment applied led to decomposition of the solid solution into pure Ag and pure Ni. In view of the equilibrium Ag-Ni phase diagram, this result is compatible with the earlier conclusion that a crystalline supersaturated Ag_xNi_{1-x} solid solution was formed by LAD.

During the above described vacuum heat treatment the resistance of the film was measured as a function of the film temperature by a four-point probe method. The result is shown in Fig. 3. Starting at a value of about 1.9 Ω at room temperature the resistance increases to a maximum value of approximately 2.3 Ω at 423 K. This resembles a normal resistance behavior of crystalline metallic materials. On continued heating the resistance decreases to about 1.3 Ω at 673 K. This is ascribed to decomposition of the solid solution: The resistance decreases as the amounts of pure Ag and pure Ni increase, because the resistivities of pure elements are substantially lower than that of a corresponding solid solution [18].

Application of the $\sin^2\psi$ analysis, as described above, yielded the following results for the stress parallel to the surface, $\sigma_\parallel$, and the strain-free lattice parameter, a_0, of the Ag_xNi_{1-x} solid solution of the 26Ag-74Ni film: $\sigma_\parallel = 0.21$ GPa and $a_0 = 3.6915$ Å. The effect of preferred orientation can be assessed for this case of a ⟨111⟩ fiber texture assuming the Reuss model for grain interaction and using the formulas of Ref. [19]. Then it follows that the value of the stress could be 25% smaller. Discussion of the value of the stress is beyond the scope of this Letter (see [5]). The value of the strain-free lattice parameter can be used to assess the composition of the solid solution. Literature values of the lattice parameters of pure Ag and pure Ni [20] are shown in a plot of the lattice parameter versus the Ag content in Fig. 4. The straight line connecting these data points represents the lattice parameter values predicted for the (metastable) solid solutions if Vegard's law prevails [21]. A lattice parameter for a metastable Ag_xNi_{1-x} solid solution has not been presented until now.

The strain-free lattice parameter of the Ag_xNi_{1-x} solid solution of the 26Ag-74Ni film, which was presented above, as well as the strained lattice parameters of the Ag_xNi_{1-x} solid solutions of this film and of the other films produced in this work have been plotted too in Fig. 4, at values of the Ag content equal to the gross Ag content of the film. Also considering the (modest) effect of the correction for the residual stress, it follows from these data that fair agreement occurs with the Vegard prediction. Hence, the average composition of the supersaturated solid solution phases in the films is approximately equal to the gross composition of the films.

The significant line broadening observed for the reflec-

tions from the solid solution, as compared to the reflections from the pure elemental components [Fig. 2(a)], can be interpreted as being caused by nonhomogeneity of the solid solution and the occurrence of microstrain and a very small crystallite size [5]. This effect can explain in particular the scatter in the data points shown in Fig. 4.

It is concluded that crystalline Ag_xNi_{1-x} solid solutions can be produced (at room temperature) by laser ablation deposition up to at least 44 at.% Ag, whereas the equilibrium solid solubility is negligible.

We would like to acknowledge Dr. K. J. A. van den Aker (Philips Centre for Materials, Technology and Innovation, Eidenhoven) for performing the $\sin^2\psi$ measurements, Dr. A. Heger (Philips Research Laboratories, Eindhoven) for provision of the four-point probe equipment, and Dr. J. J. van den Broek (Philips Research Laboratories, Eindhoven) for valuable discussions. The contributions of R. P. van Ingen and E. J. Mittemeijer are part of the research program of the Stichting voor Fundamenteel Onderzoek de Materie (Foundation for Fundamental Research on Matter).

*Present address: TNO Prins Maurits Laboratory, P.O. Box 45, 2280 AA Rijswijk, The Netherlands.

[1] J. T. Cheung and H. Sankur, CRC Crit. Rev. Solid State Mat. Sci. **15**, 63 (1988).

[2] J. F. Ready, *Effects of High-Power Laser Radiation* (Academic, London, 1971).

[3] M. F. von Allmen, *Laser-Beam Interactions with Materials,* Springer Series in Materials Science Vol. 2 (Springer-Verlag, Berlin, 1987), p. 153.

[4] J. T. Cheung and D. T. Cheung, J. Vac. Sci. Technol. **21**, 182 (1982).

[5] R. P. van Ingen, R. H. J. Fastenau, and E. J. Mittemeijer (to be published).

[6] *Thin Film Processes*, edited by C. J. Vossen and W. Kern (Academic, New York, 1980).

[7] *Binary Alloy Phase Diagrams*, edited by T. B. Massalski, H. Okamoto, P. R. Sabramamian, and L. Kacprzak (ASM International, Materials Park, OH, 1990), 2nd ed., Vol. 1, p. 64.

[8] D. Turnbull, Metall Trans. **12A**, 695 (1981).

[9] P. Duwez, ASM Trans. Q. **60**, 607 (1967).

[10] H. Jones, *Rapid Solidification of Metals and Alloys*, Monograph 8 (The Institution of Metallurgists, London, 1982).

[11] P. Duwez, R. H. Willens, and W. Klement, Jr., J. Appl. Phys. **31**, 1136 (1960).

[12] R. F. Wood and F. W. Young, Jr., in *Pulsed Laser Processing of Semiconductors*, edited by R. F. Wood, C. W. White, and R. T. Young, Semiconductors and Semimetals Vol. 23 (Academic, New York, 1984), p. 252.

[13] J. J. Hauser, Phys. Rev. B **12**, 5160 (1975).

[14] C. Vautier, J. Less-Common Met. **145**, 547 (1988).

[15] A. Muñoz, H. Miranda, F. L. Cumbrera, A. Conde, and R. Marquez, Thin Solid Films **88**, 211 (1982).

[16] R. Delhez, Th.H. de Keijser, and E. J. Mittemeijer, Surf. Eng. **3**, 331 (1987).

[17] *Smithells Metals Reference Book*, edited by E. A. Brandes (Butterworths, London, 1983), 6th ed., p. 15.2.

[18] *Handbook of Electrical Resistivities of Binary Metallic Alloys*, edited by K. Schröder (CRC Press, Boca Raton, 1983), p. 26.

[19] H. Möller and G. Martin, Mitt. K.-Wilh.-Inst. Eisenforschung **24**, 261 (1939).

[20] *Pearson's Handbook of Crystallographic Data for Intermetallic Phases*, edited by P. Villars and L. D. Calvert (ASM International, Materials Park, OH, 1991), 2nd ed., Vol. 1, p. 482; *ibid.*, 2nd ed., Vol. 4, p. 4630.

[21] J. W. Christian, *The Theory of Transformations in Metals and Alloys* (Pergamon, Oxford, 1978), 2nd ed., Pt. 1, p. 198.